Institutions of the Russian Academy of Sciences
Joint Institute for High Temperatures RAS
Institute of Problems of Chemical Physics RAS
Kabardino-Balkarian State University

Physics of Extreme States of Matter — 2010

Chernogolovka, 2010

Physics of Extreme States of Matter — 2010

Edited by academician Fortov V. E., Karamurzov B. S., Temrokov A. I., Efremov V. P., Khishchenko K. V., Sultanov V. G., Levashov P. R., Kanel G. I., Iosilevski I. L., Milyavskiy V. V., Mintsev V. B., Petrov O. F., Savintsev A. P., Shpatakovskaya G. V.

This compendium is devoted to investigations in the fields of thermal physics of extreme states of matter and physics of high energy densities. Different models and results of theoretical calculations of equations of state of matter at high pressure and temperature, physics of shock and detonation waves, experimental methods of diagnostics of ultrafast processes, interaction of intense laser, x-ray and microwave radiation, powerful ion and electron beams with matter, techniques of intense energy fluxes generation, low-temperature plasma physics, issues of physics and power engineering, and technology projects are considered. The majority of the works has been presented at the XXV International Conference on Equations of State for Matter (March 1–6, 2010, Elbrus, Kabardino-Balkaria, Russia). The edition is intended for specialists in physical and technical problems of power engineering.

The conference is sponsored by the Russian Academy of Sciences and the Russian Foundation for Basic Research (grant No. 10-02-06043).

ISBN 978-5-901675-96-0

POWER INTERACTION WITH MATTER

INVESTIGATION OF TWO-TEMPERATURE RELAXATION IN THIN FOIL ON A GLASS SUBSTRATE INITIATED BY THE ACTION OF ULTRASHORT LASER PULSE

***Khokhlov V.A.*[*1], *Inogamov N.A.*[1], *Anisimov S.I.*[1], *Zhakhovsky V.V.*[2], *Shepelev V.V.*[3], *Ashitkov S.I.*[4], *Komarov P.S.*[4], *Agranat M.B.*[4], *Fortov V.E.*[4]**

[1]*ITP RAS, Chernogolovka, Russia,* [2]*USF, Tampa, United States,* [3]*ICAD RAS, Moscow, Russia,* [4]*JIHT RAS, Moscow, Russia*

**khokhlov@landau.ac.ru*

Abstract. Under the action of ultrashort laser pulse a metal target transfers into two-temperature warm state with initial solid state density. It triggers then a chain of hydrodynamic and kinetic processes—melting, expansion, stretching, creation of tensile stress and transition into metastable state. In our case a pulse propagates through a glass substrate and illuminates an aluminum foil deposited on a glass. Several foils with different thicknesses d_f from 350 to 1200 nm have been used. The smallest thickness d_f was taken of the order of the heat penetration depth $d_T = 100$–200 nm in bulk Al. Dynamics of the d_T-layer affects the time dependence $\Delta x_{rear}(t)$ describing motion of a rear side of a foil. The d_T-layer and the rear side of a foil are coupled through acoustic waves propagating between them. We compare numerical and experimental dependencies $\Delta x_{rear}(t)$ The experimental investigations of the dynamics of rear side of foil were made using the pump-probe technique. The comparison of the results of hydrodynamics and molecular dynamics simulation with experimental data allows us shed light on the two-temperature processes occurring inside the heated layer d_T.

Introduction. Ultrashort laser pulse (UsLP) transfers near a surface layer into two-temperature warm dense matter (2T WDM) state with hot electrons: $T_e \gg T_i$, where T_e and T_i are temperatures of electron and lattice subsystems. In the 2T WDM state the electrons, firstly, have low heat capacity $C_e < C_i$ ($T_e < T_F$), and, secondly, are weakly thermally linked to the ion subsystem. Therefore their heat diffusivity χ_e, is significantly higher than the value $\chi \sim 1$ cm^2/s from reference books [5], corresponding to one-temperature conditions. Deep penetration of the electron thermal wave (EThW) $d_T \sim \sqrt{\chi_e\, t_{eq}} \sim (5-15)\delta_{skin}$ takes place during the time interval t_{eq} of the electron-ion (e-i) relaxation [1–3]. The EThW moves slow after e-i temperature equilibration.

Electron energy budget is

$$\rho D_t(E_e/\rho) = (\kappa\, T_e')' - p_e u' - \alpha\,(T_e - T_i) + Q, \quad (1)$$

where $D_t = \partial_t + u\partial_x$, $u' = \partial u/\partial x$, Q is laser energy source. The main factors in (1), defining d_T, are the coefficient α of e-i energy exchange and the heat conductivity κ, since $\kappa = \chi_e\, C_e$ and $t_{eq} \sim (T_i/T_e)C_i/\alpha$. The estimate for t_{eq} follows from the lattice energy budget $\rho D_t(E_i/\rho) = -p_i u' + \alpha\,(T_e - T_i)$, $\Delta E_i \approx C_i\,\Delta T_i$.

In our conditions F_{abs} is higher than the melting threshold F_m. Aluminum (Al) in the heated layer melts fast [1], and the thickness of the molten layer d_m is of the order of d_T. From this it follows that the depth d_T may be found from d_m. In turn, the depth d_T is defined by the coefficients α and κ in (1). In Al the coefficient $\alpha \approx 3.6\cdot 10^{18}$erg/K/cm^3/s [4] is well known. Therefore the depth d_T defines poorly known 2T thermal conductivity κ. In the work we compare simulations, using values for κ taken from [5], with results of the pump-probe experiments. Agreement between them means that the theory [5] gives right value for the coefficient $\kappa(T_e, T_i, \rho)$.

Supersonic heating and relative acoustics. It is well-known that UsLP triggers thermomechanical phenomena, see, e.g., [3, 6]. This is the case when the absorbing target is closed by a glass substrate preventing expansion of heated Al. The UsLP comes from the left side. Under compression the properties of glass SiO_2 and Al are very similar [7]. Therefore the glass-Al boundary weakly reflects acoustic wave passing through the boundary. This corresponds to the case with acoustic decay of initially motionless pressure bump into "plus" and "minus" receding waves. The width of the "plus" wave propagating to the right gives us information about the heat penetration depth d_T. The pump-probe technique pickups this information, when the wave arrives to the rear-side boundary of an Al film.

There are two new fine thermomechanical effects besides the simple well-known thermomechanical effect mentioned above (increase of pressure, formation and radiation of sonic waves from the 2T layer): (a) the imprint of the peculiarity of the Gruneisen coefficient Γ into pressure profile, and (b) formation of the tail of the "plus" wave as result of nonlinearity. The peculiarity of Γ shown in Fig. 1 is a result of melting. Difference between equilibrium and non-equilibrium melting is discussed below. The discussion is based on comparison of equilibrium 2T hydrodynamic (2T HD) calculation [1] and molecular dynamic (MD) simulation [6], which accounts for non-equilibrium melting. This peculiarity causes premature breaking of the acoustic wave, because between the two markers in Fig. 1 the dependence $p(\rho)$ is steeper than in smooth case without melting.

In case with supersonic melting the smooth passing through the inflection disappears - since there are kinks at the profile, see Fig. 2. The interval of solid-liquid mixture between the markers in Fig. 2 is the most steep. The slope at this interval becomes steeper as time goes on. This interval replaces the point of inflection. Later this interval as whole transfers to a shock. Therefore the amplitude of a shock jump shortly after

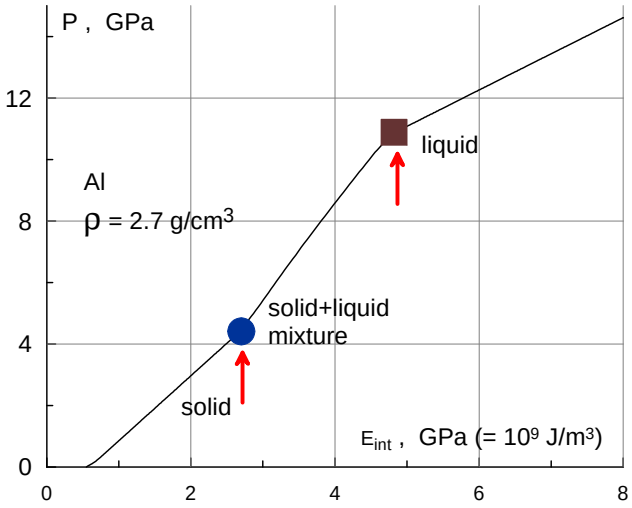

Figure 1. The kinks at the dependence $p(\rho = \text{const}, \text{E}_{\text{int}})$ are caused by equilibrium melting. The kinks imprint themselves into hydrodynamic profiles.

breaking is larger in case with fast melting in comparison with gradual growth of this amplitude from zero in case without melting. It should be emphasized that breaking takes place in the regime of acoustic propagation - significantly later after e-i equilibration.

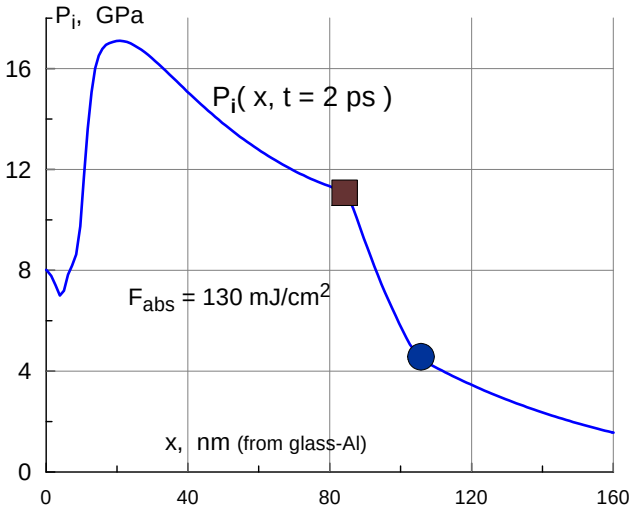

Figure 2. Ionic pressure profile at the supersonic stage of ion heating by fast EThW. The markers at the profile correspond to the markers in Fig. 1.

There is a transition from the first regime of united supersonic propagation of thermal and pressure profiles at $t < t_{eq}$ to the second regime of separate propagation of a thermal wave and a pressure wave when $t > t_{eq}$. This supersonic to sonic/subsonic pressure and thermal waves transition is shown in Fig. 3. In the first regime the electron energy E_e (1) moves through e-i transfer to an ion subsystem. This isochorically rises ionic pressure p_i. The profile in Fig. 2 corresponds to the first regime. During the united propagation the round and square markers at the pressure and melting curves in Fig. 3 coincide.

In Fig. 3 the 2T regime is confined inside the horizontal stripe t_{eq}. In this regime the curves 1 (MD, F_{abs}=82 mJ/cm^2), and two curves with markers (2T

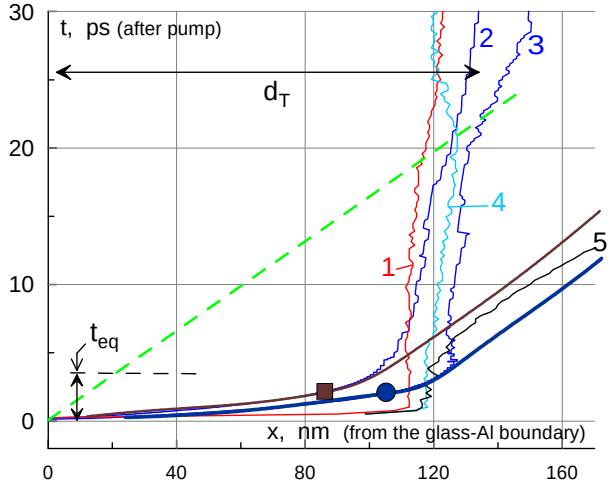

Figure 3. Radiation of the sonic perturbation by the 2T supersonic EThW when this wave transits from supersonic $t < t_{eq}$ to subsonic $t > t_{eq}$ regime. The radiation takes place when the pressure curves (the MD curve 5 and two 2T HD curves around) break away from the melting (the curves 1–3) and temperature (the curve 4, MD, $T = 1.3$kK) fronts. The curve 1 is the melting front trajectory from MD simulation. The curve with the round (square) marker corresponds to beginning (end) of melting in 2T HD. The curve 5 gives the MD isobaric trajectory for $p = 5$GPa between the markers in Figures 1 and 2. The acoustic curve 5 and two curves around carry away to the rear-side boundary the imprint of the fast melting. Pump-probe measuring of this imprint supplies us with information about 2T processes. Therein lies an acoustic probing.

HD, F_{abs}=130 mJ/cm^2) have large velocities. These curves follow the melting process. The MD curve 1 gives the isosymmetry trajectory of the symmetry index $s = 2.5$ [1]. The index measures the value of the local disorder. The value $s = 2.2$ corresponds to pure (without inclusions of pieces of unmelt lattice) liquid. The value of $t_{eq} \sim 1$ps, during which the Langevin thermostat warms up the d_T-layer, was shorter for the MD curve. In Al the duration t_{eq} is short therefore for fixed d_T the influence of this duration is small at late stage $t \gg t_{eq}$.

The dashed line in Fig. 3 presents the characteristic starting from the glass-Al boundary after arrival of the pump UsLP. Pressure in the melting zone drops down after crossing of the melting zone by this characteristic. This causes decrease of the melting temperature $T_m(\rho \approx \rho_{ini}, p)$. Therefore under high pressure the isothermal $T = 1.3$kK curve 4 is ahead the melting front 1 in Fig. 3, and the curve 4 is behind the front 1 after crossing. This means that under high pressure $T_m > 1.3$kK, while under low pressure $T_m < 1.3$kK.

Above the effect (a) with acoustic trace of fast melting has been discussed. Let us consider now the effect (b) with nonlinear tail. In linear acoustics the plus wave terminates in the characteristic starting from the point $x = 0, t = 0$. This is the dashed line in Fig. 3. In nonlinear case significant density difference appears between cold glass and hot Al as result of expansion (decay of initial jump). This causes reflection at this boundary even if we suppose that initially the glass and Al acoustic impedances are equal.

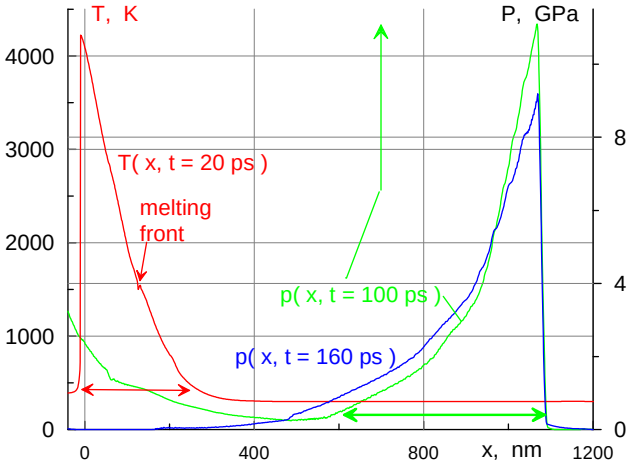

Figure 4. Extension of the pressure profile due to nonlinear reflection at the glass-Al boundary. The pressure profile is longer than the temperature profile which produces the pressure profile—compare the horizontal arrows.

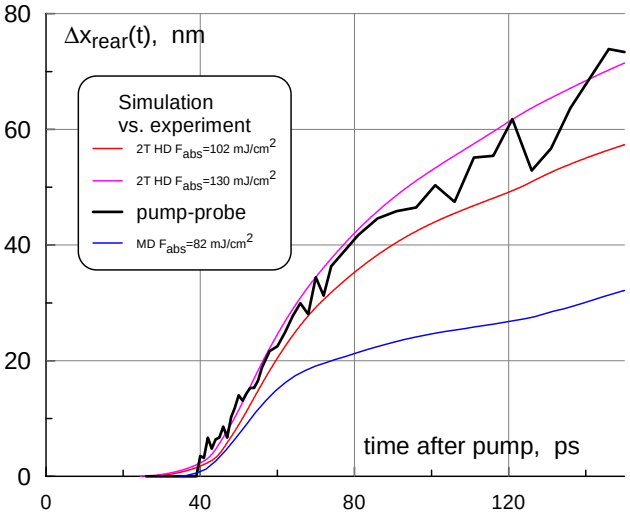

Figure 5. Transformation of pressure profile into time dependence of the shift Δx_{rear}. The Al foil thickness is 350 nm, $\tau_L = 150$fs. The F_{abs} in simulation is adjusted to fit the experimental data.

The nonlinear reflection of the minus wave at the glass-Al boundary greatly extends the width of the acoustic wave propagating to the right side. The pump-probe measurements detect this extension. The extended pressure profiles are shown in Fig. 4. The full width of the $p(x, t = 100\text{ps})$ profile is 470 nm, whereas the width of the T-profile is ≈ 270nm at the instant $t = 20$ps. At this instant the characteristic starting from the point $x = 0, t = 0$ crosses the d_T-layer, see Fig. 3. The width of the T-profile gives the width of the plus pressure wave without the tail. The two widths of the $T(x, t = 20\text{ps})$ and $p(x, t = 100\text{ps})$ are marked by the horizontal arrows.

The amplitude of the pressure tail is a measure of temperature of Al at the glass-Al boundary after e-i relaxation. In its turn, this temperature is linked to the 2T electron heat conductivity κ : since higher κ corresponds to lower temperatures. Comparison of two profiles at $t = 100$ and 160 ps is shown in Fig. 4. The profile $t = 100$ps is shifted to the position of the $p(x, t = 160\text{ps})$ profile. The maximum of the profile $t = 100$ps before the shift is marked by the vertical arrow.

Comparison of calculated and measured shift profiles is shown in Fig. 5.

Conclusions. In summary, we find two new acoustic phenomena caused by thermomechanical response to UsLP irradiation. They are the imprint of 2T supersonic melting into acoustic signal and formation of a tail due to nonlinear interaction of acoustic and entropy modes. We show that the model [5] for 2T κ describes experimental data.

The work has been supported by the RFBR grant No. 09–08–00969-a.

1. N.A. Inogamov, V.V. Zhakhovskii, S.I. Ashitkov et al., Appl. Surf. Sci. **255,** (2009) 9712; arXiv:0812.2965v1[physics.optics].
2. Wai-Lun Chan, R. S. Averback, D. G. Cahill, A. Lagoutchev, Phys. Rev. **B 78,** (2008) 214107.
3. S. Amoruso, R. Bruzzese, X. Wang et al., J. Phys. D: Appl. Phys. **40,** (2007) 331.
4. Z. Lin, L.V. Zhigilei, V. Celli, Phys. Rev. **B 77,** (2008) 075133.
5. N. A. Inogamov, Yu. V. Petrov, JETP **137,** (2010) No. 2 (in press).
6. V. V. Zhakhovskii, N. A. Inogamov et al., Appl. Surf. Sci. **255,** 9592 (2009).
7. A. V. Bushman, G. I. Kanel', A. L. Ni, V. E. Fortov, Intense dynamic loading of condensed matter, (Taylor & Francis Translation, 1993) 295 p. http://teos.ficp.ac.ru/rusbank/
8. D.J. Funk, D.S. Moore, S.D. McGrane, K.T. Gahagan et al., Thin Solid Films **453–454,** (2004) 542.
9. L. Huang, Y. Yang, Y. Wang, Z. Zheng, W. Su, J. Phys. D: Appl. Phys. **42,** (2009) 045502.

ELECTRON COLLISION FREQUENCY AND HEAT CONDUCTIVITY OF SIMPLE METALS UP TO THE ELECTRON TEMPERATURES COMPARED WITH THE FERMI TEMPERATURE

Petrov Yu. V.**, Inogamov N.A.

ITP RAS, Chernogolovka, Russia

**uvp49@mail.ru*

Introduction. When operating with two-temperature hydrodynamics equations one needs the values of parameters characterizing the target material in this state such as the electron-ion energy relaxation coefficient α_{ei}, electron heat capacity c_e, electron heat conductivity κ_e. . It is often used the phenomenological models the electron heat conductivity κ_e is presented as the combination of low temperature asymptotic value and high temperature plasma expression with taking into account the limiting value of the